

Large off-shell effects in the \bar{D}^* contribution to $B \rightarrow \bar{D}\pi\pi$ and $B \rightarrow \bar{D}\pi\bar{\ell}\nu_\ell$ decays.

Alain Le Yaouanc^a, Jean-Pierre Leroy^a and Patrick Roudeau^b

Abstract

We stress that, although the D^* is very narrow (one hundred of keV), the difference between the full D^* contribution to $B \rightarrow \bar{D}\pi\pi$ and its zero width limit is surprisingly large : several percents. This phenomenon is a general effect which appears when considering the production of particles that are coupled to an intermediate virtual state, stable or not, and it persists whether the width is large or not. The effects of various cuts and of the inclusion of damping factors at the strong and weak vertices are discussed. It is shown how the zero width limit, needed to compare with theoretical expectations, can be extracted. One also evaluates the virtual D_V^* contribution, which comes out roughly as found experimentally, but which is however much more dependent on cuts and uncontrollable "off-shell" effects. We suggest a way to estimate the impact of the damping factors.

1 Motivation

Our goal is to clarify at the same time:

1) the theoretical meaning of the measurement of $\Gamma(B \rightarrow \bar{D}^*\pi)$, i.e. how one relates the direct measurements of the quantity which we shall call Γ_3 , (which is obtained from events selected, usually, by means of a cut on the $D\pi$ mass in the 3-body $B \rightarrow \bar{D}\pi\pi$ process) to the quantity Γ_2 which characterizes the transition with the D^* considered as a stable particle, which would be a purely weak process;

2) the meaning and theoretical estimate of the measurement of the so-called D_V^* "virtual" contribution to $B \rightarrow \bar{D}\pi\pi$. This is a complementary useful process, but one whose measurement is not so well defined, and whose theoretical evaluation is less clear.

^aLaboratoire de Physique Théorique (UMR8627), CNRS, Univ. Paris-Sud, Université Paris-Saclay, 91405 Orsay, France

^bLaboratoire de l'Accélérateur Linéaire, Univ. Paris-Sud, CNRS/IN2P3, Université Paris-Saclay, Orsay, France

We first consider the $B_d^0 \rightarrow \bar{D}^0 \pi^- \pi^+$ decay channel which is simpler to interpret theoretically meanwhile our considerations are general and we study also $B^+ \rightarrow D^- \pi^+ \pi^+$ and semileptonic $B \rightarrow \bar{D} \pi \ell \nu_\ell$ decays.

2 The full contribution of \bar{D}^* to $\Gamma(B \rightarrow \bar{D} \pi \pi)$ vs the zero width limit ($g^2 \rightarrow 0$)

The aim of this section is to display the difference between the full resonance contribution of the \bar{D}^* to $B \rightarrow \bar{D} \pi \pi$ and the computation of the $B \rightarrow \bar{D}^* \pi$ decay when the \bar{D}^* is considered as a stable particle. In this section we consider a final state, $\bar{D}^0 \pi^- \pi^+$ in which the decay $D^{*-} \rightarrow \bar{D}^0 \pi^-$ is allowed, when using the nominal mass values of the particles involved. In section 4.3 we study the $D^+ \pi^- \pi^-$ final state in which the decay $D^{*0} \rightarrow D^+ \pi^-$ is forbidden, in the same conditions.

From now on we use the following notations¹:

- s : the squared invariant mass of the (would-be) resonance;
- m_1 and p_1 : the mass and the modulus of the 3-momentum of the light meson stemming from the decay of the resonance (in the resonance rest system). The corresponding 4-vector is denoted by P_1 , and a similar convention holds for the other momenta involved;
- m_2 and p_2 : the mass and the modulus of the 3-momentum of the "bachelor" light meson (in the resonance rest system);
- m_{12} : the invariant mass of the pair of pions.

In terms of the momenta of the various particles involved ("bachelor" π^+ , final \bar{D} and π^-) the amplitude for the decay chain $B_d^0 \rightarrow D^{*-} \pi^+$, $D^{*-} \rightarrow \bar{D}^0 \pi^-$ reads:

$$\begin{aligned} \mathcal{M} &= g_{D^{*-} \bar{D}^0 \pi^-} g_2 P_2^\mu \left[g_{\mu\nu} - \frac{(P_D + P_1)_\mu (P_D + P_1)_\nu}{s} \right] P_1^\nu \frac{1}{s - m_{D^*}^2 + i\sqrt{s} \Gamma_{D^*}(s)} \\ &= \frac{1}{4} \frac{g_{D^{*-} \bar{D}^0 \pi^-} g_2}{s - m_{D^*}^2 + i\sqrt{s} \Gamma_{D^*}(s)} \left[m_B^2 + m_D^2 + m_1^2 + m_2^2 - s - 2m_{12}^2 \right. \\ &\quad \left. - \frac{(m_B^2 - m_2^2)(m_D^2 - m_1^2)}{s} \right] \end{aligned} \quad (1)$$

where g_2 takes the value:

$$g_2 = G_F / \sqrt{2} V_{ud} V_{cb}^* f_\pi 2 m_{D^*} a_1 A_0(m_\pi^2) \quad (2)$$

¹ p_1 , p_2 and p'_2 are actually functions of s but we shall usually omit to write explicitly this dependence, unless their values at different energy scales must be distinguished. We shall denote by p_{1,D^*} the value of p_1 evaluated at the nominal mass of the resonance. The bachelor meson momentum in the B -meson rest system, p'_2 , is related to p_2 by $p'_2 = p_2 \sqrt{s} / m_B$.

in the factorization scheme [1]. As for $g \equiv g_{D^*-\bar{D}^0\pi^-}$, it is related to the $D^{*+} \rightarrow D^0 \pi^+$ partial width through:

$$\begin{aligned} \Gamma_{D^* \rightarrow \bar{D}^0 \pi^-}(s) &= \frac{g^2}{24\pi} \frac{1}{8s^{5/2}} [(s - (m_D - m_1)^2)(s - (m_D + m_1)^2)]^{3/2} F_R^2(s) \\ &= \frac{g^2}{24\pi} \frac{p_1^3}{s} F_R^2(s) \end{aligned} \quad (3)$$

where $F_R(s)$ is a damping factor which verifies $F_R(m_{D^*}^2) = 1$ (see below for details concerning those factors). There is some arbitrariness in the form of the Breit-Wigner (see [2, 3]). We stick to the standard formulation, advocated for instance in [7], Eq. (48.15), according to which the width in the denominator of the Breit-Wigner is energy-dependent. Thus, $\Gamma_{D^*}(s)$ is the total width of the resonance taken at the invariant mass \sqrt{s} . This choice corresponds to what is called BW_δ in [4] which discusses those matters in detail; $-i\sqrt{s}\Gamma(s)$ is precisely the absorptive part of the self-energy generated by the $D\pi$ loop calculated through Feynman graphs (see Appendix 3).

A related ambiguity occurs regarding the numerator of the resonance Breit-Wigner. In this note we use the form $g_{\mu\nu} - \frac{(P_D+P_1)_\mu(P_D+P_1)_\nu}{s}$ instead of the $g_{\mu\nu} - \frac{(P_D+P_1)_\mu(P_D+P_1)_\nu}{m_{D^*}^2}$ one suggested by the isobaric model². When estimated in terms of resonance rest frame quantities, the expression inside the square brackets in Eq. (1) (which stems from the first form above) reduces to $4p_1 p_2 \cos(\theta)^3$ as expected (see for example [5] and [6]) and assumed by the experimental analyses, see in particular the D_V^* .

Had we used the second form, an extra term would have appeared, namely $4g g_2 \frac{m_{D^*}^2 - s}{m_{D^*}^2 s} (m_B^2 - m_2^2 - s)(m_D^2 - m_1^2 - s)$. This quantity does not depend on m_{12} and, consequently, will show no dependence on $\cos(\theta)$. This is due to the fact that the propagator is no longer transverse when the resonance is off-shell, i.e., it has a scalar part in addition to the spin-1 component. The extra term vanishes at the resonance mass but could give a relatively more important contribution at the upper end of the phase-space. However this would concern the S-wave and, since we are interested here in the P-wave channel, we keep the other form.

It is customary, in experimental papers, to introduce damping factors in the analyses, the so-called "Blatt-Weisskopf" functions, although their exact meaning is not precisely stated. These functions have been introduced in nuclear physics and used for particles emitted at very low momenta within a quantum mechanical potential-well description of the nucleus; therefore it is not clear whether they can be used in high energy reactions. In the theoretical formula for \mathcal{M} above this amounts to introducing two functions $F_B(s)$ and $F_R(s)$, leading to

²By isobaric model we mean effective field-theoretic models including vector fields describing spin one resonances and subject to Feynman rules, see for instance the treatment of the Δ by Gourdin and Salin [22].

³ θ is the angle between the 3-momenta of the two pions, in the resonance rest-frame.

$$\mathcal{M}' = \frac{1}{4} \frac{g g_2 F_B(s) F_R(s)}{s - m_{D^*}^2 + i\sqrt{s} \Gamma_{D^*}(s)} \left[m_B^2 + m_D^2 + m_1^2 + m_2^2 - s - 2m_{12}^2 - \frac{(m_B^2 - m_2^2)(m_D^2 - m_1^2)}{s} \right] \quad (4)$$

It may be reminded that the expression for $\Gamma_{D^*}(s)$ contains the term $F_R^2(s)$ (see Eq. (3)). Those factors depend on s through the momenta p_2 (or p_2') and p_1 . By convention the value of the damping factors is 1 when the resonance is "on-shell" but, as we shall see, their influence is not negligible as one integrates the (squared) amplitude over s to get Γ_3 . According to Blatt and Weisskopf, for the case we are interested in of a vector resonance, F_R takes the form $F_R(s) = \sqrt{(1 + (r_{BW} p_{1,D^*})^2)/(1 + (r_{BW} p_1)^2)}$. The form of F_B is similar except for the substitution of p_1 by either p_2 (*LHCb*) or p_2' (*CLEO and B-factories*). This dependence introduces an extra parameter generically denoted by " r_{BW} " in the following⁴ and consequently an extra source of uncertainty.

Going back to expression (1), leaving aside any contribution besides the resonance and squaring the amplitude one gets for the resonant contribution to the 3-body decay width:

$$\Gamma_3 \equiv \Gamma_{(B_d^0 \rightarrow D^{*-} \pi^+; D^{*-} \rightarrow \bar{D}^0 \pi^-)} = \frac{g^2 g_2^2}{(2\pi)^3} \frac{1}{256 m_B^3} \int \frac{ds dm_{12}^2}{(s - m_{D^*}^2)^2 + s \Gamma_{D^*}^2(s)} F_R^2(s) \times F_B^2(s) \left[m_B^2 + m_D^2 + m_1^2 + m_2^2 - s - 2m_{12}^2 - \frac{(m_B^2 - m_2^2)(m_D^2 - m_1^2)}{s} \right]^2 \quad (5)$$

The final integration with respect to the invariant mass of the pions leads to

$$\Gamma_3 = \frac{g_2^2 g^2}{192 \pi^3} \int_{(m_D + m_1)^2}^{(m_B - m_2)^2} \frac{ds}{s^{3/2}} \frac{F_B^2(s) p_2'^3(s) F_R^2(s) p_1^3(s)}{(s - m_{D^*}^2)^2 + s \Gamma_{D^*}^2(s)} \quad (6)$$

which can be rewritten as

$$\Gamma_3 = \frac{1}{\pi} \int_{(m_D + m_1)^2}^{(m_B - m_2)^2} ds \frac{\Gamma_{B_d^0 \rightarrow D^{*-} \pi^+}(s) s^{1/2} \Gamma_{D^{*-} \rightarrow \bar{D}^0 \pi^-}(s)}{(s - m_{D^*}^2)^2 + s \Gamma_{D^*}^2(s)} \quad (7)$$

Thus, using the general formula

$$\delta(x) = \frac{1}{\pi} \lim_{\epsilon \rightarrow 0} \frac{\epsilon}{x^2 + \epsilon^2}$$

one immediately gets:

$$\lim_{\Gamma_{D^*} \rightarrow 0} \Gamma_3 = \Gamma_{B_d^0 \rightarrow D^{*-} \pi^+}(m_{D^*}^2) \times BR \quad (8)$$

⁴Actually there are two parameters, since there is no a-priori reason why the two damping factors should be identical.

with $BR \equiv BR_{D^{*-} \rightarrow \bar{D}^0 \pi^-}(m_{D^*}^2)$ the branching ratio in the channel under consideration, taken at $\sqrt{s} = m_{D^*}$ by virtue of the δ function.

The value of the 2-body decay width is:

$$\Gamma_2 \equiv \Gamma_{B_d^0 \rightarrow D^{*-} \pi^+}(m_{D^*}^2) = \frac{g_2^2}{8\pi} \frac{1}{m_{D^*}^2} p_2'^3(m_{D^*}^2). \quad (9)$$

3 Numerical aspects: dependence on the D^* width

3.1 Dependence on g^2 at fixed D^* mass

In this section we measure the effect of changing the value of the g coupling constant by introducing a scaling parameter λ so that g^2 is changed into $\lambda \times g^2$ or, equivalently, $\Gamma_{D^* \rightarrow D\pi}(s)$ goes to $\Gamma_{D^* \rightarrow D\pi}(s, \lambda) \equiv \lambda \times \Gamma_{D^* \rightarrow D\pi}(s)$. We change the *total* width in the denominator in the same way so that the partial and total widths are both scaled proportionally⁵, getting:

$$\Gamma_3(\lambda) = \frac{1}{\pi} \int_{(m_D+m_1)^2}^{(m_B-m_2)^2} ds \Gamma_{B_d^0 \rightarrow D^{*-} \pi^+}(s) \frac{\lambda s^{1/2}}{(s - m_{D^*}^2)^2 + \lambda^2 s \Gamma_{D^*}^2(s)} \Gamma_{D^* \rightarrow \bar{D}^0 \pi^-}(s) \quad (10)$$

and we define $R(\lambda) \equiv \Gamma_3(\lambda) / (\Gamma_2 \times BR)$.

Letting λ vary from 0 to 1, one should get in the $\lambda \rightarrow 0$ limit the result announced in the preceding section (zero-width limit), $\lim_{\lambda \rightarrow 0} R(\lambda) = 1$ while for $\lambda = 1$ one recovers the physical situation.

In Figure 1 we show the behavior of $R(\lambda)$. The numerical values are taken from the Particle Data Group Review [7] and the coupling constants are fitted from the two-body decay widths formulae in order to reproduce their experimental values without referring to a specific decay mechanism we get: $g = 16.8$, see Appendix 2, $a_1 A_0 = 0.576$, see Eq. (13)⁶. It is seen that the behavior is linear and that the deviation from unity is rather large, of the order of 10% at the physical value $\lambda = 1$, although the D^* is still very narrow. The inclusion of the B-meson Blatt-Weisskopf factor (i.e. at the weak vertex), results in an enhancement of the ratio, while, on the contrary, the resonance damping induces a strong depletion. We recall that the various groups (namely CLEO/B-factories and LHCb) use different definitions for the damping factors. Clearly, using the LHCb definition strongly increases the effect, even though both conventions lead to qualitatively similar effects: at the physical point ($\lambda = 1$) it amounts to a several percent effect.

3.2 Dependence on m_{D^*} at fixed coupling constant

In the previous subsection we have considered the behaviour of $R(\lambda)$ at fixed m_{D^*} as g goes to zero. Meanwhile, the value of g is determined by the strong

⁵Strictly speaking, this procedure is not fully correct since there is no reason why the various channels contributing to the total width should scale in the same way.

⁶Note, however, that our discussion is fully independent of those numerical values.

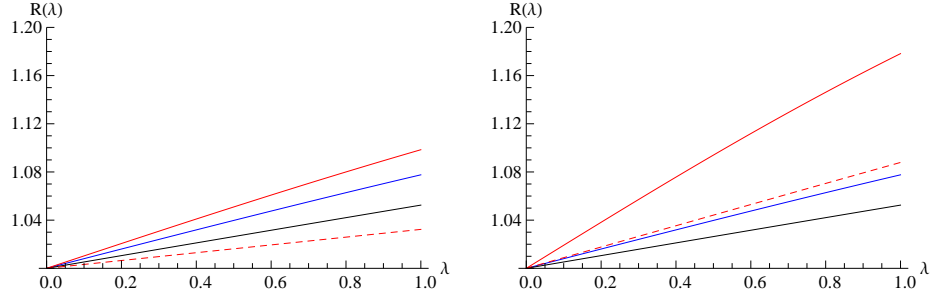


Figure 1: Behavior of $R(\lambda)$ as function of λ and effect of the "Blatt-Weisskopf" damping factors:

- full line, blue: without any damping factor,
- full line, black: with the resonance damping only,
- full line red: with the B-meson damping only,
- dashed, red: with both dampings.

On the left, the damping factor F_B is evaluated using the momentum of the bachelor particle computed in the B rest frame whereas, on the right, it is evaluated in the resonance rest frame. The parameter r_{BW} is taken to be 1.6 GeV^{-1} in both cases.

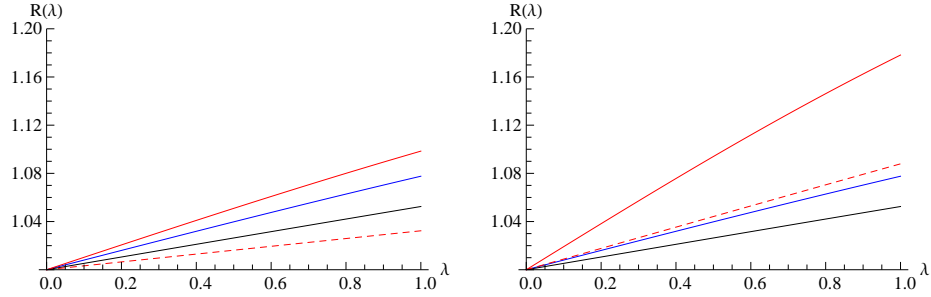


Figure 2: same as Figure 1 with $r_{BW} = 4 \text{ GeV}^{-1}$ in both cases.

interaction and is independent of the mass to first approximation. Therefore, since the nominal D^* width is proportional to $g^2 p_{1,D^*}^3$, one has to consider also the limit at fixed g , letting p_{1,D^*} , and consequently the width, go to zero. Such a limit is obtained by lowering the mass of the resonance so that it becomes close to threshold. This corresponds to the actual situation for the D^* , whose narrowness is only due to the proximity of its mass to the threshold.

Figures 3 and 4 show the behavior of $R(1)$ as a function of the resonance mass. It is seen that, whatever damping scenario is considered, $R(1)$ remains fairly constant and significantly different from 1 when the resonance-mass varies from threshold to 2.1 GeV , which corresponds to a variation of the width from 0 to 7 MeV . When the mass gets close to the threshold, the low mass part of the

resonance peak shrinks to 0, which means that the departure from 0 is mainly due to the real part of the propagator. This is similar to the effect of the N -pole in $N - \pi$ scattering.

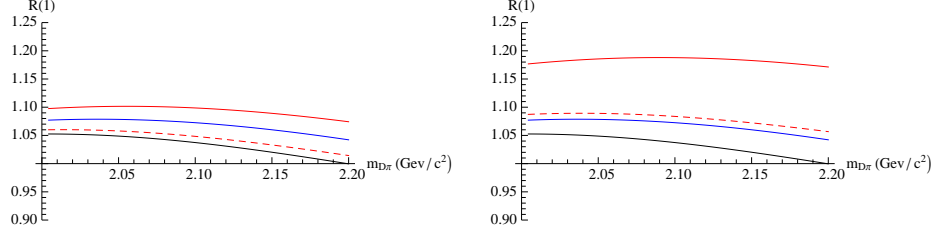


Figure 3: Behavior of $R(1)$ as a function of the mass $m_{D\pi}$ of the resonance. The conventions are the same as in Figure 1.

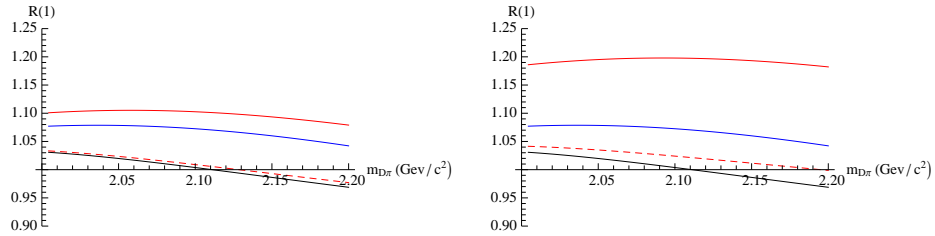


Figure 4: same as Figure 3 with $r_{BW} = 4 \text{ GeV}^{-1}$.

4 Comparison with experiment in hadronic B decays

One now turns to the question of relating above calculations to experimental observations. As explained in previous sections, we have to distinguish:

- 1 the zero width limit Γ_2 , which is a theoretical concept describing the rate $\Gamma_{B_d^0 \rightarrow D^{*-} \pi^+}$ as a decay to two stable particles. This is the quantity which can be compared with corresponding theoretical computations.
- 2 the width obtained in 3-body decays, Γ_3 , which uses $\bar{D}^0 \pi^- \pi^+$ events belonging to the decay $B_d^0 \rightarrow D^{*-} \pi^+$, $D^{*-} \rightarrow \bar{D}^0 \pi^-$ and is obtained by fitting the corresponding decay rate over all the available phase space.

In Particle Decay Tables [7] the quantity Γ_3 is generally used when quoting decay branching fractions of heavy mesons into 3-body states, in which two of the emitted particles come from an intermediate resonance.

The decay $B_d^0 \rightarrow D^{*-}\pi^+$ is peculiar because a large fraction of the $\bar{D}^0\pi^-$ mass distribution is concentrated over a small interval, which contains the D^{*-} mass and, usually, only events which belong to such an interval are selected to measure $BR(B_d^0 \rightarrow D^{*-}\pi^+)$. Unfortunately, different experiments are using different mass intervals ($\pm 3, < 10 \text{ MeV}/c^2$ by reference to m_{D^*} or $m(D\pi) < 2.1 \text{ GeV}/c^2$) and it is not clear to understand, from present publications, how (or even if) corrections are done, using simulated events, to account for the presence of D^* decays outside the selected range (apart for resolution effects that are corrected). Therefore one needs a precise definition of what is called a D^* in experimental measurements to be able to combine results obtained in different analyses and have a clear link with phenomenology when using simulated events. We detail this recommendation in Section 4.1. It must be reminded that the $B \rightarrow \bar{D}^*\pi$ decay channel is used at LHC to normalize different measurements and it is important to minimize uncertainties on this quantity.

On the other hand the tail of the D^* extends up to large $D\pi$ mass values, with distances from the pole mass that are thousands times larger than the width of the resonance. In effect, as we have explained in Section 3, the behaviour of the D^* tail is similar to the one expected for other resonances, with a higher mass. It is simply the D^* intrinsic width which is very small due to the proximity of m_{D^*} with the decay channel threshold. Once the D^* peak is eliminated by a cut on the $D\pi$ mass or when the $D\pi$ threshold has a higher value than m_{D^*} , only the tail of the D^* , named D_V^* , contributes in $D\pi\pi$ analyses. This component is usually fitted without using any information relating its rate and mass dependence to expectations from the D^* tail. This point is discussed in Section 4.2 by comparing present D_V^* measurements and expectations.

4.1 The $B_d^0 \rightarrow D^{*-}\pi^+$ decay channel

Measurements from Belle [8] and BaBar [9, 10] collaborations are based on a small fraction of their registered statistics and their results are not in good agreement.

From the publications it is not clear if quoted branching fractions are restricted to a given mass range centered on the D^{*-} mass or if measurements are corrected, using a simulation, to correspond to $BR(B_d^0 \rightarrow D^{*-}\pi^+)$ over the total available phase-space?

Leaving aside these remarks and using values from [7] we obtain:

$$BR(B_d^0 \rightarrow D^{*-}\pi^+) \times BR = (1.855 \pm 0.089) \times 10^{-3}. \quad (11)$$

with $BR \equiv BR(D^{*-} \rightarrow \bar{D}^0\pi^-)$ as in previous sections. The value for $a_1 A_0$, is obtained in the zero width approximation limit, by comparing this value to the corresponding expectation:

$$BR_2(B_d^0 \rightarrow D^{*-}\pi^+) \times BR = \frac{\Gamma_2 \tau_{B_d^0}}{\hbar} BR. \quad (12)$$

Using the expression for Γ_2 given in Eq. (9), this gives:

$$a_1 A_0 = 0.576 \pm 0.014. \quad (13)$$

4.1.1 Comparing our expectations and experimental results

Taking into account the finite width of the D^{*-} , expected values for $BR(B_d^0 \rightarrow D^{*-}\pi^+) \times BR$ are obtained by integrating the $B_d^0 \rightarrow \bar{D}^0\pi^-\pi^+$ partial decay width, given in Eq. (5) over several $\bar{D}^0\pi^-$ mass intervals. Therefore we define:

$$BR_3 = \frac{\Gamma_3 \tau_{B_d^0}}{\hbar} = BR_3(m < m_{cut}) + BR_3(m > m_{cut}) \quad (14)$$

In these evaluations, the value of $a_1 A_0$, obtained in the zero D^{*-} width approximation, and given in Eq. (13), is used.

A relativistic Breit-Wigner distribution is used to describe the D^* resonance:

$$R_{D^*} = \frac{1}{s - m_{D^*}^2 + i\sqrt{s}\Gamma_{D^*}(s)} \quad (15)$$

with

$$\Gamma_{D^*}(s) = \sum_{i=1}^{\infty} \Gamma_{D^*}^i \left(\frac{p_1^i}{p_{1,D^*}^i} \right)^3 \left(\frac{m_{D^*}}{\sqrt{s}} \right)^2 F_R^2(p_1^i). \quad (16)$$

as seen from Eqs. (1) and (3) or Eq. (47.18) of [7]. The value of m_{D^*} is the resonance mass and $\Gamma_{D^*}^i$ is its partial decay width for the i channel. p_1^i and p_{1,D^*}^i are the breakup momenta at the mass $m = \sqrt{s}$ and m_{D^*} respectively. The damping factor F_R is equal to unity at $m = m_{D^*}$. It decreases the tail at large mass values of the resonance and gives some enhancement below m_{D^*} . In the present analysis two parameterizations are used for the damping factor. The one derived from a model proposed for nuclear physics by Blatt and Weisskopf and another parameterization [11], used at B-factories in analyses containing a D^* , and which corresponds to an exponential distribution:

$$F_R(p_1^i) = e^{-\alpha(p_1^i - p_{1,D^*}^i)}. \quad (17)$$

For D^{*+} decays, we consider that the index i varies between 1 and 3 and corresponds to the channels $D^0\pi^+$, $D^+\pi^0$, and $D^+\gamma$ respectively. We have not considered additional decay channels that should be present at high masses.

Results are given in Table 1; the considered $m_{D\pi}$ intervals are those used in Belle [8], BaBar [12] and LHCb [13] in their analyses of the $B_d^0 \rightarrow \bar{D}^0\pi^-\pi^+$ 3-body decay channel. Values considered for r_{BW} or α are representative of those measured in different experiments, as indicated in the last column of Table 3.

When integrating over the whole Dalitz plane (second line), the expected branching fraction decreases by about 5% when α varies between 0 and $4 (GeV/c)^{-1}$. This variation is reduced below the 2 permil level if, for example, a mass range of $\pm 10 MeV/c^2$ is used to select D^{*-} candidates.

Therefore, if the D^{*-} production is measured within a fixed mass range, around the D^{*-} mass, comparison with theoretical expectations, obtained in the same conditions, can be of high accuracy and are not dependent on the parameterization of damping form factors.

r_{BW} or α (GeV/c) ⁻¹	0	1.6	4.0
no mass cut	1.998	1.930	1.890
	1.998	1.966	1.914
$\Delta m < 3 \text{ MeV}/c^2$	1.840	1.840	1.840
	1.840	1.840	1.840
$\Delta m < 10 \text{ MeV}/c^2$	1.855	1.854	1.853
	1.855	1.855	1.855
$m(D^0\pi^-) < 2.1 \text{ GeV}/c^2$	1.887	1.880	1.873
	1.887	1.886	1.882

Table 1: Values for $BR_3(m < m_{cut}) = BR(B_d^0 \rightarrow D^{*-}\pi^+) \times BR \times 10^3$ obtained for different choices of the mass range around the D^{*-} mass and using an exponential (first line) or the Blatt-Weisskopf parameterization (second line) for the damping factors. The theoretical expression, obtained in the zero width approximation, is normalized to data to fix the value of the parameter $a_1 A_0$. The value for $BR_2(B_d^0 \rightarrow D^{*-}\pi^+) \times BR$ is 1.855×10^{-3} (Eq.(11)). It can be noted that $BR_3(m < m_{cut})$ branching fractions are almost independent of the value of the damping parameter, r_{BW} or α , once the measurement is done within a given mass range, meanwhile their values depend on the chosen mass interval.

Ratios between expected widths in different mass intervals and the value obtained in the narrow width approximation are independent of $a_1 A_0$.

$$R(m_{cut}) = \frac{\Gamma_3(m < m_{cut})}{\Gamma_2 \times BR} \quad (18)$$

Without any cut on the $\bar{D}^0\pi^-$ mass, this ratio changes from 1.077 if no damping form factors are included and 1.020 using form factors with an exponential dependence and $\alpha = 4 \text{ (GeV}/c)^{-1}$. This variation comes from the tails in the mass distribution, outside the D^{*-} region. Restricting the mass interval to $\Delta m < 10 \text{ MeV}/c^2$, the ratio is equal to unity and variations observed by considering different hypotheses on damping factors are at the permil level.

We note also a variation of 2.5% on the value of the branching fraction when considering the three mass intervals given in Table 1 and used by different experiments. This quantifies the importance of quoting the limits of the Δm interval over which the branching fraction is evaluated by the various analyses.

It is also possible to define the cut (m_{cut}^0) on the $\bar{D}^0\pi^-$ mass so that the corresponding integrated three body decay branching fraction corresponds to the value expected from theory in the zero width approximation. It is independent of the value of the form factor $a_1 A_0$ and almost also of the damping factors:

$$m_{cut}^0 = m_{D^*} + (9 - 10) \text{ MeV}/c^2 \quad (19)$$

These results are obtained with the momentum of the bachelor pion, which enters in $F_B(p)$, computed in the B meson rest frame, as was done at B-factories.

This aspect is developed in section 4.2.

4.1.2 Proposal to quote $BR(B_d^0 \rightarrow D^{*-}\pi^+)$

To avoid uncertainties related to the unknown shape of damping form factors and to account for effects related to the choice of the m_{cut} value, we advocate to quote $BR(B_d^0 \rightarrow D^{*-}\pi^+)$ for events selected within a specified $m_{D\pi}$ interval. Measured quantities have to be corrected for different experimental effects, using simulated events, but no correction must be applied to account for the cut on $m_{D\pi}$ (apart for resolution effects) so that corrected events correspond only to those situated in the quoted mass interval before any experimental effect.

If experiments use different intervals in $m_{D\pi}$ it is necessary to correct individual measurements so that they correspond to the same mass range, before computing the average.

The obtained value will then be essentially independent of hypotheses for damping factors if the combinatorial background, present under the D^* , in the selected mass interval, can be estimated in a way which does not depend much on the high mass tail of the signal. To compare with theory, the value m_{cut}^0 , given in Eq. (19), is adequate.

4.2 Rate and branching fraction for the virtual contribution $B_d^0 \rightarrow \bar{D}_V^{*-}\pi^+$

The measured fraction of $B_d^0 \rightarrow \bar{D}_V^{*-}\pi^+$ events in the 3-body $B_d^0 \rightarrow \bar{D}^0\pi^-\pi^+$ final state, after vetoing the D^* mass region ($m_{D\pi} > m_{cut}$), is of the order of 10 % and is concentrated at low $\bar{D}^0\pi^-$ mass values.

4.2.1 Theoretical expectations for the D_V^{*-} component

In Table 2, values for $BR_3(m > m_{cut}) = BR(B_d^0 \rightarrow D_V^{*-}\pi^+) \times BR(D_V^{*-} \rightarrow \bar{D}^0\pi^-)$ are obtained using the value of $a_1 A_0$ previously determined and for two parameterizations of damping form factors. In the following we use the notation : $BR_V \equiv BR(D_V^{*-} \rightarrow \bar{D}^0\pi^-)$ because this quantity can have a value different from BR , which was defined at the resonance mass.

Results given in the first two lines, for each mass range, are obtained using the value of the bachelor pion momentum, which enters in the damping factor $F_B(p)$, computed in the B rest frame. If, instead, we use the corresponding momentum value obtained in the $D\pi$ rest frame we get the results given in the third line. In this case, one notes that, for $r_{BW} = 1.6 (GeV/c)^{-1}$, branching fractions are higher than without damping. This effect was also apparent in Figure 1. Such differences are obtained using the Blatt-Weisskopf parameterization and we observe that using an exponential distribution gives much more dramatic differences: the D_V^{*-} component increases by more than one hundred times. These effects are not usually mentioned in publications because they are not present, neither in B-factories analyses, as they take the bachelor pion momentum evaluated in the B rest frame, nor in LHCb which uses the resonance

r_{BW} or α (GeV/c) ⁻¹	0.0	1.6	3.0	4.0	5.0
$\Delta m > 3 MeV/c^2$	1.578	0.899	0.615	0.499	0.420
		1.256	0.893	0.742	0.638
		1.769	1.131	0.900	0.751
$\Delta m > 10 MeV/c^2$	1.427	0.753	0.476	0.363	0.288
		1.105	0.743	0.594	0.492
		1.617	0.980	0.751	0.604
$m(D^0\pi^-) > 2.1 GeV/c^2$	1.111	0.494	0.254	0.165	0.110
		0.797	0.456	0.326	0.244
		1.297	0.682	0.473	0.346

Table 2: $BR_3(m > m_{cut}) = BR(B_d^0 \rightarrow D_V^{*-} \pi^+) \times BR_V \times 10^4$ expectations for different values of the damping parameter and of the selected mass range. For each mass range, the first line corresponds to the exponential parameterization of the damping form factor, the second line is obtained with the Blatt-Weisskopf parameterization and the third line uses the same parameterization but the bachelor pion momentum is computed in the resonance rest frame.

rest-frame but does not use any exponential form factor distribution. It can be shown that, if the bachelor pion momentum is evaluated in the B rest frame, then the product $F_R(p_1) \times F_B(p_2)$ goes to one for large $D\pi$ masses (if the same function is used for F_R and F_B) whereas it can take arbitrary large values if p_2 is evaluated in the resonance rest frame.

Let us recall that there are no really compelling theoretical arguments for the introduction of the Blatt and Weisskopf damping factors, and even less for choosing such or such momentum dependence. However results are sensitive to them as can be concluded, for instance, from Table 2 and this constitutes a source of uncertainty. Our present conclusion, considering this arbitrariness in the parameterization of damping factors, is to consider that the bachelor pion momentum, that enters in F_B , has to be evaluated in the B rest frame. If the value of the damping parameter, r_{BW} , used in F_B , is smaller than the one that enters in F_R , the total damping will be lower than unity at large $m_{D\pi}$. This indicates also that dedicated studies are needed to measure directly these form factors.

4.2.2 Experimental measurements of the D_V^{*-} component

Measurements obtained by Belle, BaBar and LHCb collaborations are compared with expectations in Table 3 and in Figure 6. These values are extracted from Table 2 using corresponding values for r_{BW} and α .

In the Belle analysis, only statistical uncertainties were quoted. The variation range for r_{BW} (and α), between 0 and $3(GeV/c)^{-1}$ is chosen to illustrate the sensitivity of theoretical expectations on the value of this parameter.

In the BaBar measurement, the dominant uncertainty comes from the pa-

Experiment	$BR(B_d^0 \rightarrow D_V^{*-} \pi^+) \times BR(D_V^{*-} \rightarrow \bar{D}^0 \pi^-) \times 10^4$	our evaluation (exponential/Blatt-Weisskopf)	r_{BW} or α (GeV/c) $^{-1}$
Belle [8]	0.88 ± 0.13 (<i>no syst.</i>)	$0.90^{+0.68}_{-0.28} / 1.26^{+0.32}_{-0.37}$	$1.6^{+1.4}_{-1.6}$
BaBar [12]	$1.39 \pm 0.08 \pm 0.16 \pm 0.35 \pm 0.02$	$0.36^{+0.12}_{-0.07} / 0.59^{+0.15}_{-0.10}$	4 ± 1
LHCb [13]	$0.78 \pm 0.05 \pm 0.02 \pm 0.15$	$0.49 / 0.79$	1.60 ± 0.25

Table 3: Measurements of D_V^* components in $B_d^0 \rightarrow \bar{D}^0 \pi^- \pi^+$ decays are compared with expectations. The latter are provided for two choices of the damping factor parameterization, exponential and Blatt-Weisskopf respectively and using central values and uncertainties on α or r_{BW} quoted by corresponding experiments (apart for Belle for which we use a variation between 0 and 3 (GeV/c) $^{-1}$).

parameterization of the $\bar{D}^0 \pi^-$ S-wave, in the threshold region, including a “dabba” component.

In the LHCb measurement, the quoted uncertainty on r_{BW} is very small when compared with previous determinations, meanwhile it does not include any systematic uncertainty on this parameter⁷.

From Table 3 it appears that measured and expected values for the D_V^* component are compatible, as already observed by Belle [8]. Meanwhile experimental uncertainties remain quite large (those from LHCb being underestimated) and are difficult to estimate because they are mainly of theoretical origin, being dependent on the assumed value for r_{BW} (or α) and on hypotheses for the variation of the damping factor with $m_{D\pi}$. It must be noted also that the value of the D_V^* component is dominated by the low mass region.

4.2.3 Expected variation of the D_V^{*-} component with $m_{D\pi}$

Experiments have usually assumed a relativistic Breit-Wigner distribution for the D_V^{*-} component (Belle, BaBar). In the LHCb analysis [13], an arbitrary distribution is fitted on data:

$$R(s) = e^{-\beta_1(s-5.4)-i\beta_2(s-5.7)}. \quad (20)$$

This distribution has two problems to describe a D_V^{*-} component: a very fast fall-off versus $m_{D\pi}$ and an unexpected phase variation (the D_V^{*-} amplitude is expected to be real and the phase to be constant, away from m_{D^*}). But no experiment has really measured the D_V^{*-} lineshape.

It has to be noted that the expected mass distribution is almost independent of the exact value of the D^* total decay width. This is illustrated in Figure 5 from which it can be concluded that the D_V^* mass distribution is the one expected from a simple pole, modified by damping form factors.

⁷The value of r_{BW} measured by LHCb cannot be directly compared with previous determinations because, in LHCb, the damping $F_B(p)$ is evaluated using the momentum (p) computed in the resonance rest frame instead of using the B rest frame.

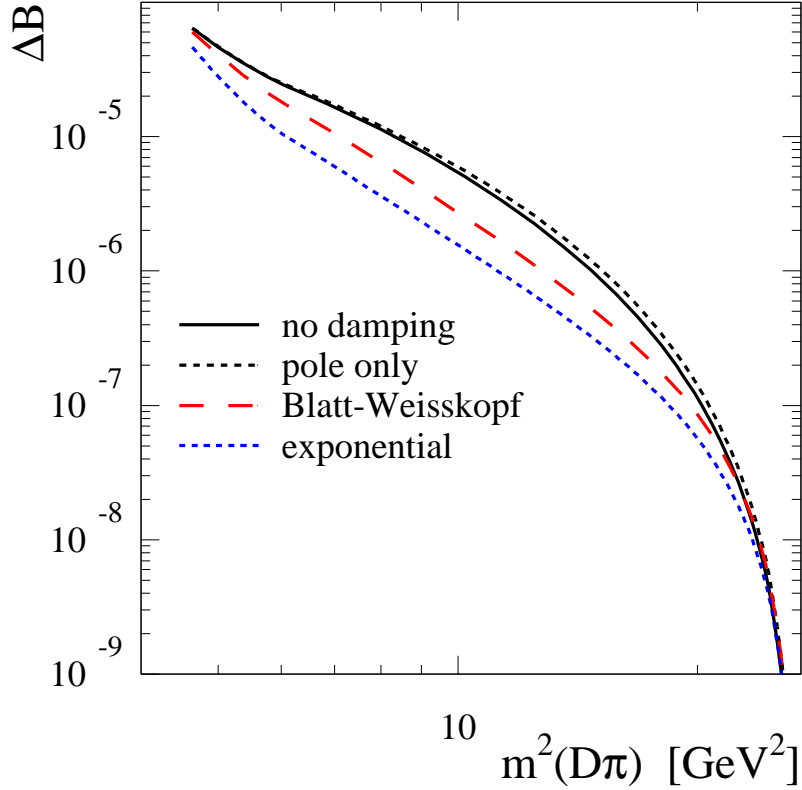


Figure 5: Comparison between the expected variation of the D_V^{*-} component versus $m^2(D\pi)$ for different choices of damping form factors. The black full line is obtained without damping whereas Blatt-Weisskopf (red line) and exponential (blue line) damping factors are used, with the same value for the parameter (α or $r_{BW} = 1.6 (\text{GeV}/c)^{-1}$). The black dashed line is obtained assuming that the total D^* decay width is equal to zero (therefore, in this case, the D^* amplitude is of course real). Some difference is observed at large masses ($m^2(D\pi) > 10 (\text{GeV}/c^2)^2$) which becomes non-visible, once some damping is present. ΔB is the expected branching fraction in a bin. There are 20 equal-size bins between $(2.02 \text{ GeV}/c^2)^2$ and $(m_B - m_\pi)^2$.

We display, in Figure 6, comparisons between D_V^* distributions fitted by experiments and our expectations. The latter are obtained with the exponential parameterization of damping factors and we use $\alpha = 1.6 (GeV/c)^{-1}$.

It has to be reminded that our evaluations are based on the D^* production in the mass region of the resonance and are therefore absolutely normalized. The distribution obtained in Belle is compatible with our expectation. The agreement in rate is not trivial. Meanwhile, for the mass variation, we have used the same parameterization (exponential with $\alpha = 1.6 (GeV/c)^{-1}$) as favored by Belle. BaBar and LHCb observe a higher rate at low mass values.

Because the distribution is essentially fixed by the D^* pole, even in the presence of damping factors, we consider that the D_V^* component has a non negligible contribution at large masses. Therefore the fitted distribution by LHCb, with a fast fall-off, is not physical.

4.3 The $B^- \rightarrow D^+ \pi^- \pi^-$ decay channel

The LHCb collaboration has obtained a high statistics measurement of the decay $B^- \rightarrow D^+ \pi^- \pi^-$ [14]. Previous compatible results were obtained by Belle [11] and BaBar [15] collaborations but systematic uncertainties were not provided on the D_V^* component. Experimentally this channel has the interest, when compared with $B^0 \rightarrow \bar{D}^0 \pi^- \pi^+$ that, the $\pi^- \pi^-$ final state being exotic, the decay amplitude is easier to parameterize and the analysis is more sensitive to the various components in the $D\pi$ final state. Meanwhile, for theory, this decay is more difficult to interpret, being of Class III. But, independently of any theoretical prejudice, it is possible to verify if the measured D_V^* component:

$$BR(B^- \rightarrow D_V^{*0} \pi^-) \times BR(D_V^{*0} \rightarrow D^+ \pi^-) = (1.09 \pm 0.07 \pm 0.07 \pm 0.24 \pm 0.07) \times 10^{-4} \quad (21)$$

is compatible with the tail expected from the D^{*0} .

In this comparison we use the measured contribution of the D^{*0} in the decay $B^- \rightarrow D^{*0} \pi^-$, $D^{*0} \rightarrow D^0 \pi^0$, with a branching fraction equal to $(4.90 \pm 0.17) \times 10^{-3} \times (64.7 \pm 0.9) \times 10^{-2} = (3.17 \pm 0.12) \times 10^{-3}$ [7].

We have computed the corresponding decay rate by integrating the square of the decay amplitude modulus, given in Eq. (22), over the $D^0 \pi^0 \pi^-$ phase space, restricting the $D^0 \pi^0$ mass interval to values below $m_{D\pi} < 2.020 GeV/c^2$ to isolate the D^{*0} meson.

$$\mathcal{A} = C R_{D^*}(m) F_B(p_2') F_R(p_1) T_1(p_2, p_1, \cos(\theta)) \quad (22)$$

As already discussed in Section 4.2, this expression differs from the one used by LHCb in the evaluation of the damping F_B for which we take the momentum of the bachelor pion computed in the B rest frame in place of the resonance frame.

The value of the normalization factor (noted C) is then determined such that this evaluation corresponds to the measured value.

To obtain the D_V^* contribution in the $B^- \rightarrow D^+ \pi^- \pi^-$ decay channel we assume that it comes from the decay chain: $B^- \rightarrow D^{*0} \pi^-$, $D^{*0} \rightarrow D^+ \pi^-$. The

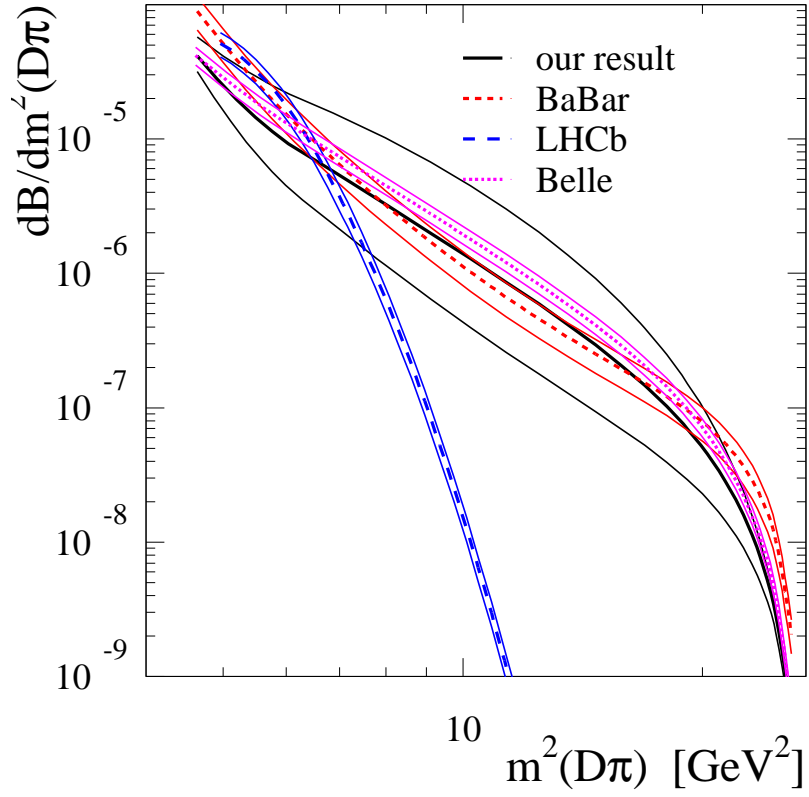


Figure 6: Comparison between fitted D_V^{*-} components, in BaBar, Belle and LHCb (dashed lines), with our expectation. For the latter, we use exponential damping factors with $\alpha = 1.6 (\text{GeV}/c)^{-1}$ (full line), while the thin black lines on each side of the expectation are obtained by changing the value of α between 0. and $3. (\text{GeV}/c)^{-1}$. Thin lines drawn for each of fitted experimental curves correspond to quoted uncertainties on D_V^* , given in publications.

decay threshold having a higher value than $m_{D^{*0}}$, it is not possible to compute the value of the decay momentum, at the resonance mass, which enters in the expression of the partial decay width given in Eq. (16). In such circumstances, usually, an effective mass is introduced in published analyses, which has a value much higher than the threshold. Measurements of the corresponding D_V^* component are essentially independent of this choice, mainly because fractions and not absolute decay rates are measured. In practice, if one takes the expression for the mass dependent decay width, as given in Eq. (3) which does not refer to the decay width at the resonance mass, it is not needed to use any effective mass. As for damping factors, we take them equal to unity at the decay threshold.

The decay amplitude is symmetrized because there are two possible $D^+\pi^-$ mass values, noted respectively $m_{min.}$ and $m_{max.}$.

$$A_{D_V^*} = \mathcal{A}(m_{min.}) + \mathcal{A}(m_{max.}) \quad (23)$$

where the amplitude $\mathcal{A}(m)$ is given in Eq. (22). The expected decay rate is obtained by integrating $C^2|A_{D_V^*}|^2$ over the plane defined by the variables $m_{min.}^2$ and $m_{max.}^2$.

The values given in Table 4 are obtained for different hypotheses on the α or r_{BW} parameters and using the exponential and the Blatt-Weisskopf parameterizations for $F_{B,R}$.

r_{BW} or α (GeV/c) ⁻¹	0.0	2.0	3.0	4.0	5.0
$BR(B^- \rightarrow D_V^{*0}\pi^-)$	2.81	0.68	0.43	0.30	0.22
$\times BR(D_V^{*0} \rightarrow D^+\pi^-) \times 10^4$	2.81	1.77	1.27	0.98	0.78
	2.81	2.86	1.89	1.37	1.06

Table 4: $BR(B^- \rightarrow D_V^{*0}\pi^-) \times BR(D_V^{*0} \rightarrow D^+\pi^-) \times 10^4$ expectations for different values of the damping parameter. The bachelor pion momentum, entering in the F_B damping, is computed in the B rest frame in the second and third lines, and in the resonance frame in the last one. In the second line the exponential parameterization is used whereas for the two other lines we take the Blatt-Weisskopf expression.

Using the parameterization of LHCb with $r_{BW} = (4 \pm 1) (GeV/c)^{-1}$, which is the value they assume for this parameter, their measurement in Eq. (21) has to be compared with our estimate given in the last line of Table 4: $1.4_{-0.3}^{+0.6} \times 10^{-4}$.

5 The $\bar{B} \rightarrow [D\pi]\ell\bar{\nu}_\ell$ final state

Similarly to what we have done for hadronic decays, we consider two regions in the $D^* \rightarrow D\pi$ mass distribution. The low mass region is used to measure the D^* component which plays an important role in the determination of the $|V_{cb}|$ parameter. At higher masses, the tail of the D^* mass distribution is noted D_V^* , as in previous sections. The component, denoted as $[D\pi]_{broad}$, corresponds to

experimental measurements of $D\pi$ final states, after a cut on $m_{D\pi}$ and from which $D_2^* \rightarrow D\pi$ decays are subtracted. The interpretation of these $[D\pi]_{broad}$ events in terms of physical components has been problematic for a long time. It has been most often considered that they are coming from $D_0^* \rightarrow D\pi$ decays but this has not been established experimentally and does not agree with theoretical predictions [16]. From theory it is expected that narrow states are produced at a larger rate than broad states because $\tau_{3/2}(1) > \tau_{1/2}(1)$, where $\tau_{3/2}(w)$ and $\tau_{1/2}(w)$ are the Isgur-Wise form factors [20] and w is the product of the 4-velocities of the B and D mesons, and additionally because of kinematical factors. Numerically, the expected branching fractions are an order of magnitude higher for narrow states whereas the experimental value:

$$BR(\bar{B}_d^0 \rightarrow [D\pi]_{narrow}\ell\bar{\nu}_\ell) = (0.18 \pm 0.02) \% \quad (24)$$

is lower than the corresponding value for broad states, obtained by averaging Belle [17] and BaBar [18, 19] measurements:

$$BR(\bar{B}_d^0 \rightarrow [D\pi]_{broad}\ell\bar{\nu}_\ell) = (0.42 \pm 0.06) \% \quad (25)$$

Computations of $BR(\bar{B} \rightarrow [D\pi]_{broad}\ell\bar{\nu}_\ell)$ were done by several authors in the framework of heavy quark and chiral symmetries [21, 23, 24, 26]. They obtain a broad component which can be large but their predictions vary over a wide range depending on their definition for the resonant component and on the cut on the soft pion momentum. We have not used their detailed expressions for the decay branching fraction and considered that the contribution from the D^* pole is dominant, as they had observed. Our approach differs also because the coupling constant g has now been accurately measured and because we give a well defined scheme to compare experimental measurements with theoretical predictions. We have found that the value expected for the D_V^* component of the D^* resonance is compatible with the $[D\pi]_{broad}$ measurements. Therefore, the broad contribution is perhaps neither, as previously considered, the D_0^* one, which should be very small, nor one coming from a radial excitation, as also suggested [27], but the D_V^* one. An excess of events at low $D\pi$ mass values is observed in Belle and BaBar analyses but the helicity distribution measured by Belle does not favor the D_V^* hypothesis. Meanwhile present statistics are too low to provide definite conclusions. Measurements of higher values for $\bar{B} \rightarrow D^*\ell^-\bar{\nu}_\ell$ branching fractions obtained by fitting the inclusive lepton momentum distribution as compared with those obtained with exclusive analyses may point also to some missing D_V^* component [28, 29]?

5.1 $\bar{B} \rightarrow D^*\ell^-\bar{\nu}_\ell$

The semileptonic decay width for this reaction is used to measure the CKM parameter $|V_{cb}|$ by comparing the corresponding experimental branching fraction with theoretical expectations, obtained in the hypothesis that the D^* is a stable particle.

Integrating over decay angles, the partial decay width depends on two variables: $m_{D\pi} = \sqrt{s}$ and w , the latter being related to q^2 , the invariant "squared mass" of the two-lepton system:

$$w = \frac{m_B^2 + s - q^2}{2m_B\sqrt{s}}. \quad (26)$$

If one assumes that the D^* is stable, then $m_{D\pi} = m_{D^*}$ and the differential decay width becomes, in analogy to what was found in the nonleptonic case:

$$\frac{d\Gamma}{dw} = \frac{G_F^2 m_B^3}{48\pi^3} r^3 (m_B - m_{D^*})^2 \chi(w) \eta_{EW}^2 \mathcal{F}^2(w) |V_{cb}|^2 \quad (27)$$

where $r = m_{D^*}/m_B$. The form factor $\mathcal{F}(w)$ depends on three form factors and is usually expressed in terms of one of them $-h_{A_1}(w)$ - and of the ratios $-R_1(w)$, $R_2(w)$ - of the two others relative to $h_{A_1}(w)$.

$$\begin{aligned} \chi(w) \mathcal{F}^2(w) = & h_{A_1}^2(w) \sqrt{w^2 - 1} (w + 1)^2 \left\{ 2 \left[\frac{1 - 2wr + r^2}{(1 - r)^2} \right] \left[1 + R_1^2(w) \frac{w - 1}{w + 1} \right] \right. \\ & \left. + \left[1 + (1 - R_2(w)) \frac{w - 1}{1 - r} \right]^2 \right\}. \end{aligned} \quad (28)$$

We use the parameterization of [25] for the functions that enter in Eq. (28):

$$\begin{aligned} h_{A_1}(w) &= h_{A_1}(1) [1 - 8\rho^2 z + (53\rho^2 - 15)z^2 - (231\rho^2 - 91)z^3], \\ R_1(w) &= R_1(1) - 0.12(w - 1) + 0.05(w - 1)^2, \\ R_2(w) &= R_2(1) + 0.11(w - 1) - 0.06(w - 1)^2 \end{aligned} \quad (29)$$

where $z = (\sqrt{w + 1} - \sqrt{2})/(\sqrt{w + 1} + \sqrt{2})$. The values obtained by the HFAG group [30] for the parameters, ρ^2 , $R_1(1)$, and $R_2(1)$, that enter in Eq. (29) are the following:

$$\rho^2 = 1.205 \pm 0.026, \quad R_1(1) = 1.404 \pm 0.032, \quad \text{and} \quad R_2(1) = 0.854 \pm 0.020. \quad (30)$$

They have been determined from a fit to experimental data that includes also the normalization for the decay rate:

$$\eta_{EW} \mathcal{F}(1) |V_{cb}| = (35.61 \pm 0.43) \times 10^{-3}. \quad (31)$$

Using these values, we have verified that, integrating Eq. (27) over w , to obtain the semileptonic decay partial width of the B_d^0 meson, we recover the central value of 4.88 % for the corresponding measured decay branching fraction which is given by HFAG. Corresponding central values for the semileptonic decay width into a D^* , considered as a stable particle, are respectively for the neutral and the charged B meson:

$$\Gamma_2^{sl}(B_d^0) = 2.113 \times 10^{-14} \text{ GeV} \quad \text{and} \quad \Gamma_2^{sl}(B^-) = 2.116 \times 10^{-14} \text{ GeV}. \quad (32)$$

The small difference between these two values is attributed to differences in the masses of the particles involved.

5.1.1 Virtual D^* contribution

To evaluate the effects induced by the D^* coupling to the $D\pi$ final state, one multiplies Eq. (27) by:

$$R^i(s) = \frac{1}{\pi} \frac{\sqrt{s}\Gamma_i(s)}{(s - m_{D^*}^2)^2 + (\sqrt{s}\Gamma_{D^*}(s))^2} \quad (33)$$

where the index "i" refers to the relevant decay channel. In the limit $\Gamma_{D^*}(s) \rightarrow 0$, this expression corresponds to $\delta(s - m_{D^*}^2)$ and one recovers Eq. (27) multiplied by the branching fraction of the D^* into the i decay channel ($\mathcal{B}_i = \Gamma_i(m_{D^*})/\Gamma_{D^*}(m_{D^*})$). Total and partial widths include the Blatt-Weisskopf damping factor F_R . By tradition, the F_B damping term is not used when computing semileptonic decays.

We have included three decay channels of the D^* : $D^0\pi^+$, $D^+\pi^0$, and $D^+\gamma$ for the charged state and $D^0\pi^0$, $D^+\pi^-$, and $D^0\gamma$ for the neutral one. If we integrate over s and w , values for the semileptonic decay widths, Γ_3^{sl} , divided by Γ_2^{sl} , are given in Table 5 (we have adopted the same notation as for hadronic B decays: the index 2 refers to a stable D^* particle):

$r_{BW} (GeV/c)^{-1}$	0	1	1.85	3	5
$B_d^0 \rightarrow D^{*+}e^-\bar{\nu}_e$	1.089	1.072	1.056	1.041	1.028
$B^- \rightarrow D^{*0}e^-\bar{\nu}_e$	1.085	1.068	1.052	1.038	1.025

Table 5: *Partial decay widths for the channel $\bar{B} \rightarrow D^*e^-\bar{\nu}_e$ relative to the values obtained for a stable D^* meson. The first line gives the value (in $(GeV/c)^{-1}$ units) of the parameter r_{BW} , used in the Blatt-Weisskopf damping factor.*

Depending on the value of the damping parameter, the semileptonic partial width obtained by integrating over the D^* mass distribution exceeds by 3 to 9 % the value obtained in the zero width approximation. This is a situation similar to the decay $B \rightarrow \bar{D}^*\pi$ studied in Section 4.1.

The mass interval, centered on m_{D^*} , which is such that the integral restricted over this interval is equal to Γ_2^{sl} corresponds to $\Delta_3(m) = \pm(9-10) MeV/c^2$ and the obtained partial width is almost independent of the value of the damping parameter (with relative variations $< 10^{-3}$).

To obtain the value for $|V_{cb}|$ one needs the value of $\mathcal{F}(1)$ and this quantity is evaluated for a stable D^* particle. Therefore we consider that theoretical expectations have to be compared with the measured branching fraction restricted to the interval $\Delta_3(m)$. The event simulation must not be used to correct for D^* decays that are outside this interval. One difficulty is to fix the level of the combinatorial background under the D^* signal, in the $\Delta_3(m)$ mass interval, because the D^* signal is still present at large $D\pi$ masses and its exact contribution depends on damping factors and on the opening of other decay channels. It is therefore important to have a better experimental control of the so called D_V^* mass distribution. In present publications there is usually some missing

information to understand exactly how measurements were done. It would be nice if the different experimental collaborations would clarify this situation.

5.2 $\bar{B} \rightarrow D_V^* \ell^- \bar{\nu}_\ell$

As we have noted, in previous sections, the D_V^* component is not negligible in $\bar{B}_d^0 \rightarrow D^0 \pi^+ \pi^-$ decays where it corresponds to about 10% of remaining events, once the D^* peak is excluded. It is peaked at low $D\pi$ mass values and it extends over a large mass range.

To evaluate the branching fraction for $\bar{B}_d^0 \rightarrow D_V^{*+} \ell^- \bar{\nu}_\ell$ we have integrated the differential decay width $d^2\Gamma/dw ds$ over w and s for $\sqrt{s} > m_{D^*} + 9 \text{ MeV}/c^2$ (by comparison, in Belle, they select events with $\sqrt{s} > m_{D^*} + 1.5 \text{ MeV}/c^2$ whereas BaBar uses $\sqrt{s} > m_D + 180. \text{ MeV}/c^2$).

$r_{BW} (\text{GeV}/c)^{-1}$	0	1	1.85	3	5
$\bar{B}_d^0 \rightarrow D_V^{*+} e^- \bar{\nu}_e$	0.48	0.38	0.29	0.21	0.14
$B^- \rightarrow D_V^{*0} e^- \bar{\nu}_e$	0.49	0.39	0.29	0.21	0.13

Table 6: *Estimated semileptonic branching fractions (in %) for the channel $\bar{B} \rightarrow D_V^* e^- \bar{\nu}_e$. The first line gives the value (in $(\text{GeV}/c)^{-1}$ units) of the parameter r_{BW} , used in the Blatt-Weisskopf damping factor.*

Therefore, comparing the values given in Table 6 with the measurement from Eq. (25), it appears that the D_V^* component can explain all or a large fraction of the “missing” decay channel in $\bar{B}_d^0 \rightarrow [D\pi]_{\text{broad}} \ell \bar{\nu}_\ell$.

In addition, the D_V^* component can be identified experimentally because it has characteristic $m_{D\pi}$ (see Fig. 7) and angular distributions. Therefore, B hadron semileptonic decays offer a nice opportunity to study the $D\pi$ mass distribution of the D_V^* component because of the absence of any additional hadron in the decay final state. Such measurements can be considered at LHCb because present statistics from B-factories published analyses are too low for such studies.

6 Conclusions

We have found that, to compare expected branching fractions with experiment in $\bar{B} \rightarrow D^* \pi$ and $\bar{B} \rightarrow D^* \ell \bar{\nu}_\ell$ decays, that are always provided from theory in the zero width limit, one has to integrate the $D^* \rightarrow D\pi$ mass distribution from threshold up to $m_{\text{cut}}^0 = m_{D^*} + (9 - 10) \text{ MeV}/c^2$ (Eq. 19); this interval corresponds to more than one hundred times the intrinsic resonance width. In this way, the two values are expected to agree at the permil level, independently of effects from damping factors that are usually introduced in decay amplitudes (see Table 1). Such an accuracy supposes a precise control of the $D\pi$ combinatorial background level, within the selected mass range. This is a priori non trivial because of the presence of D^* decays at high mass values (the so-called

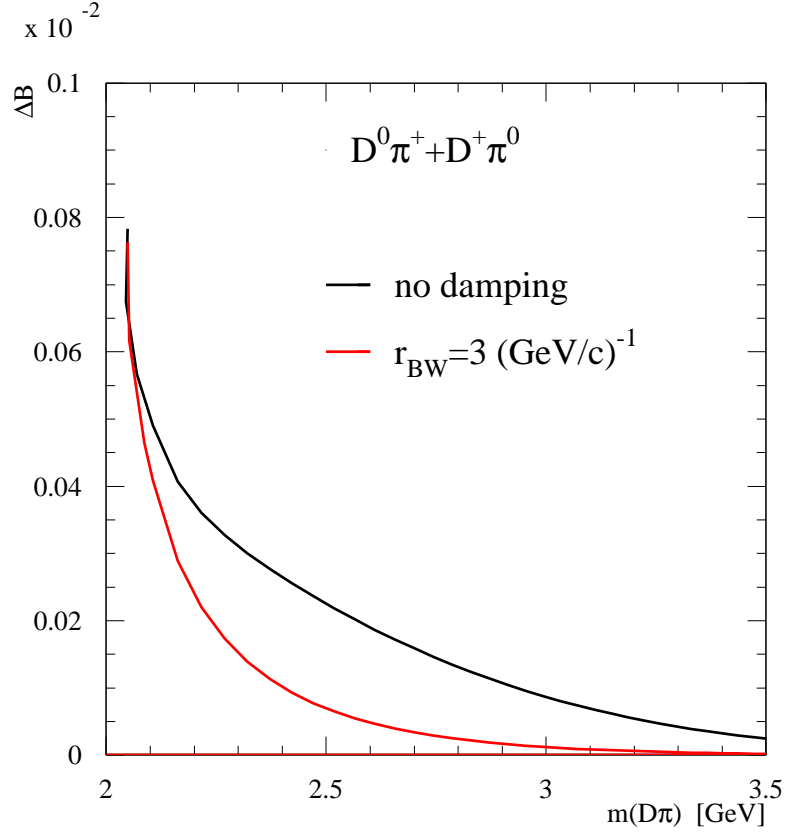


Figure 7: *Expected $D\pi$ mass distribution for the D_V^* component in \bar{B}_d^0 hadron semileptonic decays. The two curves, correspond to expectations without damping (black) and with (red) using the Blatt-Weisskopf distribution with $r_{BW} = 3 \text{ (GeV/c)}^{-1}$. ΔB is the branching fraction expected in each $m_{D\pi}^2$ bin. There are 100 equal-size bins between $(m_{D^{*+}} + \Delta_3)^2$ and $m_{B_d^0}^2$.*

D_V^* events) that need to be estimated. Therefore it is also important to have a good understanding of this component.

The D_V^* component corresponds to $m(D\pi) > m_{cut}^0$ and comes mainly from the real part of the D^* propagator. We have shown that its relative importance, when compared with the zero width limit, is essentially independent of the value of the vector resonance intrinsic width (see section 3.2) when this quantity is computed according to $\Gamma_0 \propto g^2 p_0^{*3}$, the coupling g being a constant fixed by strong interactions. This result is verified by changing the mass of an hypothetical vector resonance, decaying into $D\pi$, between threshold and $2.1 \text{ GeV}/c^2$, which corresponds to Γ_0 varying between ~ 0 and 7 MeV . We find that the measured D_V^* production rate is compatible with expectations obtained from the D^* within uncertainties that are quite large at present (see Table 3). Specifically, predicted branching fractions depend on the parameterization of damping factors and on the way they are computed (see Table 2). In this note we have not really addressed some aspects that can still affect the D_V^* evaluation, such as: the physical origin and interpretation of damping factors, and the opening of new decay channels at large masses.

We therefore consider that it is important to have an experimental control of the D_V^* component. The $B^- \rightarrow D^+ \pi^- \pi^-$ seems promising in this respect because large statistics can be analyzed and no resonance is expected in the two-pion channel (see Section 4.3). Another appealing possibility is the semileptonic $\bar{B} \rightarrow D\pi\ell\bar{\nu}_\ell$ decay because of the absence of a third hadron in the final state and because the D_V^* component is expected to dominate the $D\pi$ channel (see Section 5).

Acknowledgements

We would like to thank V. Tisserand and Wenbin Qian for providing us with some details about the $B_d^0 \rightarrow \bar{D}^0 \pi^- \pi^+$ decay measurement in LHCb. We thank in particular T. Gershon and T. Latham for answering several questions we had on $\bar{B} \rightarrow D\pi\pi$ analyses in BaBar. Comments from B. Kowalewski on a possible D_V^* contribution to explain the difference between inclusive and exclusive measurements of the $\bar{B} \rightarrow D^* \ell^- \bar{\nu}_\ell$ branching fraction are included. We have also commented searches for the D_V^* component in exclusive semileptonic decays done in BaBar and Belle experiments, as suggested by M. Rotondo.

Appendix 1: An illustrative model

We use a simplified model to display the physical origin of the relatively large difference existing between the partial decay widths Γ_3 and $\Gamma_2 \times BR$, in spite of the extreme smallness of Γ_{D^*} . The main simplifications are that

- 1) we discard any damping factor;

- 2) in the denominator of the propagator, we consider a fixed width Γ_{D^*} depending only on the D^* mass instead of $\Gamma(s)$, which would be more respectful of unitarity.

Differences between this simplified model and numerical results quoted in the article, that were obtained using a variable decay width, do not seem essential. The magnitude of the effect is the same as in the more complete calculation.

The expression for Γ_3 is given in Eq. (6). It can be rewritten:

$$\Gamma_3 = C \int_{(m_D+m_\pi)^2}^{(m_B-m_\pi)^2} ds \frac{\phi(s)}{(s-m_{D^*}^2)^2 + (m_{D^*}\Gamma_{D^*})^2} \quad (34)$$

The constant C is some combination of numerical factors and coupling constants not relevant here since we discuss only ratios. The function $\phi(s)$ is equal to:

$$\phi(s) = \frac{p_2'^3(s) p_1^3(s)}{s^{3/2}}. \quad (35)$$

In the zero D^* width limit one gets the equality⁸:

$$\lim_{\Gamma_{D^*} \rightarrow 0} \Gamma_3 = \Gamma_2 \times BR = C\pi\phi(m_{D^*}^2)/(m_{D^*}\Gamma_{D^*})$$

The intermediate expression in the equation above corresponds to $\Gamma_{B_d^0 \rightarrow D^*-\pi^+} \times BR$ in Eq. (8).

To display the difference between Γ_3 and its limit, one may rewrite $\pi\phi(m_{D^*}^2)/(m_{D^*}\Gamma_{D^*})$ as the integral:

$$\int_{(m_D+m_\pi)^2}^{(m_B-m_\pi)^2} ds \frac{\phi(m_{D^*}^2)}{(s-m_{D^*}^2)^2 + (m_{D^*}\Gamma_{D^*})^2} \quad (36)$$

This is an approximation, but a very good one. It amounts to replace $\frac{\pi}{m_{D^*}\Gamma_{D^*}}$ (which is the exact result for the same integral, but with infinite bounds) by:

$$\frac{\pi}{m_{D^*}\Gamma_{D^*}} \left[1 - \frac{m_{D^*}\Gamma_{D^*}}{\pi A} - \frac{m_{D^*}\Gamma_{D^*}}{\pi B} \right] \quad (37)$$

where $A = m_{D^*}^2 - (m_D + m_\pi)^2$ and $B = (m_B - m_\pi)^2 - m_{D^*}^2$.

The relative difference between the Γ_3 and $\Gamma_2 \times BR$ decay widths is then equal to:

$$\begin{aligned} R - 1 &= \frac{\Gamma_3 - \Gamma_2 \times BR}{\Gamma_2 \times BR} \\ &\simeq m_{D^*}\Gamma_{D^*} \frac{1}{\pi\phi(m_{D^*}^2)} \int_{(m_D+m_\pi)^2}^{(m_B-m_\pi)^2} ds \frac{\phi(s) - \phi(m_{D^*}^2)}{(s-m_{D^*}^2)^2 + (m_{D^*}\Gamma_{D^*})^2} \end{aligned} \quad (38)$$

In the factors in front of the integral, the critical dependence of Γ_{D^*} on the m_{D^*} mass through the factor $p_1^3(m_{D^*}^2)$ (see Eq. (3)) which could lead one to

⁸We recall that BR stands for $BR_{D^* \rightarrow \bar{D}^0 \pi^-}(m_{D^*}^2)$.

believe that the expression tends to zero at threshold, is compensated exactly by the same factor in $\phi(m_{D^*}^2)$. Displaying explicitly the coupling constant factor, and taking into account that the above expression involves the total width Γ_{D^*} instead of the partial one given in Eq. (3) ($BR \approx 2/3$), one ends with:

$$R - 1 \approx \frac{1}{16\pi} g_{D^*D\pi}^2 m_{D^*}^2 \frac{1}{\pi p_2^3(m_{D^*}^2)} \int ds \frac{\phi(s) - \phi(m_{D^*}^2)}{(s - m_{D^*}^2)^2 + (m_{D^*} \Gamma_{D^*})^2}, \quad (39)$$

One sees that there remains only a smooth dependence on m_{D^*} in $p_2^3(m_{D^*}^2)$ (B decay) and from the integral, as observed in the numerical curves of subsection 3.2. In particular, the limit $m_{D^*} \rightarrow m_D + m_\pi$ is finite and $\neq 0$, although the width goes to 0.

The magnitude of $R - 1$ is controlled by the magnitude of the coupling constant: it is roughly proportional to $g_{D^*D\pi}^2$. One would recover $R \approx 1$ if this coupling was very small, as shown in the beginning of the paper. But of course it is not small in reality. The smallness of the D^* width is accidental, only due to the proximity to the threshold, and the coupling is comparable to the one for other strong couplings like $g_{NN\pi}$. Numerically, one finds for the physical value of $g_{D^*D\pi}^2$ and for m_{D^*} very close to the threshold, in fact for an arbitrarily small width, $R - 1 \approx 0.09$.

Appendix 2: The Determination of the $g_{D^*D\pi}$ coupling constant

The value of $g_{D^*-D^0\pi^-}$ is obtained from the measurement of the D^{*+} hadronic decay width using the expression given in Eq. (3).

Experiments have measured the total width of the D^{*+} meson and the small contribution from electromagnetic decays needs to be subtracted to obtain the hadronic component. Using values quoted in [7] this gives:

$$\Gamma_{D^{*+} \rightarrow D\pi}^{expt.} = (83.4 \pm 1.8) \times (1 - 0.016 \pm 0.004) keV = (82.1 \pm 1.8) keV. \quad (40)$$

It corresponds to:

$$g_{D^*D\pi}^{expt.} = 16.81 \pm 0.18. \quad (41)$$

This value is obtained using the hypothesis of I-spin symmetry to relate the $D^0\pi^+$ and $D^+\pi^0$ decay channels of the D^{*+} , taking into account the difference of the decay momenta. The validity of this hypothesis can be checked by comparing the measured $(67.7 \pm 0.5)\%$ and expected $(67.6 \pm 0.3)\%$ values for $BR_{D^{*+} \rightarrow D^0\pi^+}$.

Appendix 3: On the s -dependence of the imaginary part of the resonance propagator

In this Appendix we want to demonstrate the statements and claims formulated in the text about the s dependence of $-i\sqrt{s} \Gamma(s)$, i.e. of the imaginary part

of the self-energy, namely that it is proportional to $\frac{1}{\sqrt{s}}$ times the usual factors $q(s)^{2l+1}$, for an l decay partial wave⁹, $q(s)$ being the decay momentum for a particle of mass \sqrt{s} in its rest frame. This conclusion is obtained by using a loop model.

Basis of the calculation

For the sake of simplicity, we shall make our demonstration for the case of a scalar resonance of mass M decaying into two identical scalars of mass m . The extension to the case of a vector resonance like the D^* is straightforward.

The propagator can be written as:

$$\frac{1}{s - M^2 - \Sigma(s)} \quad (42)$$

with $s = p^2$ and $\Sigma(s)$ is the self energy contribution, having in fact obviously a dimension *mass squared*. We are here only interested in the imaginary part of $\Sigma(s)$, although there is of course also a real s -dependent mass shift. In the literature, this imaginary (absorptive) part is either denoted as $-i\sqrt{s} \Gamma(s)$ or $-iM\Gamma_M(s)$. Note that in the beginning this is only a matter of convention, if the quantities $\Gamma_M(s)$ or $\Gamma(s)$ are evaluated accordingly, with $M \Gamma_M(s) = \sqrt{s} \Gamma(s)$, from the same imaginary part, but it may be a source of confusion. The justification of such notations is just to explicit the dimension of a *mass squared* and to recall the relation with the physical width, let us say, which would be defined at the pole mass. In fact, as is obvious in the calculation, the absorptive cannot depend on the mass M , but only on s and m , so that the notation $-iM\Gamma(s)$ introduces a dependence on M in both factors which is rather artificial. We therefore stick to the notation $-i\sqrt{s} \Gamma(s)$.

Now the only simple way to get an explicitly covariant expression for $-i\sqrt{s} \Gamma(s)$ in accordance with the analyticity and unitarity requirements of field theory is to use Feynman diagrams and to generate the self-energy and its imaginary part by the loop contributions, which are produced by iteration of the (normal ordered) coupling of the M particle to the two identical others:

$$\lambda : \Phi_M (\phi_m)^2 : \quad (43)$$

with λ the (dimensionful) coupling constant to appear also in the decay width, and Φ_M, ϕ_m the fields corresponding to the respective scalar particles. We therefore proceed by applying the standard Feynman rules to the calculation of the corresponding propagator.

⁹This differs from the expressions given in the new section "48. Resonances" in the 2018 edition of PDG [7], Eqs. (48.22) and (48.23), where it is only $\propto q(s)^{2l+1}$.

Calculation

Let P be the momentum entering the loop and $s = P^2$. The self-energy is generated by the series of loop diagrams:

$$\frac{i}{s - M^2} \sigma \frac{i}{s - M^2} + \frac{i}{s - M^2} \sigma \frac{i}{s - M^2} \sigma \frac{i}{s - M^2} + \dots \quad (44)$$

with σ coming from the loop integral:

$$\sigma = \frac{i^2 \lambda^2}{2} \int \frac{d^4 K}{(2\pi)^4} \frac{i^2}{(K^2 - m^2)((P - K)^2 - m^2)} \quad (45)$$

The factors in front of the integral come from twice the vertex $i\lambda$, and a factor $1/2$ for the bosonic loop. These loop contributions, added to the bare $i \frac{1}{s - M^2}$, give:

$$\frac{i}{s - M^2 - \Sigma(s)}, \quad (46)$$

with $\Sigma = i\sigma(s)$, whence finally:

$$\Sigma = i \frac{\lambda^2}{2} \int \frac{d^4 K}{(2\pi)^4} \frac{1}{(K^2 - m^2)((K - P)^2 - m^2)} \quad (47)$$

It is obvious that Σ does not contain any dependence on the mass M of the decaying scalar.

We need only the absorptive part of Σ , which we obtain by means of the Cutkosky rule, i.e. the substitution:

$$\frac{1}{u - m^2} \rightarrow 2\pi i \delta(u - m^2) \quad (48)$$

for each denominator $u - m^2$ inside the loop. The calculation is easily done in the frame where $\vec{p} = 0$, yielding:

$$-2i\sqrt{s} \Gamma(s) = Disc \Sigma = \frac{i\lambda^2}{2} \left(-\frac{1}{4\pi} \frac{q(s)}{\sqrt{s}} \right) \quad (49)$$

$$\Gamma(s) = \frac{1}{2} \frac{\lambda^2}{8\pi} \frac{q(s)}{s} \quad (50)$$

with $q(s) = \frac{1}{2}\sqrt{s - 4m^2}$, i.e. the decay momentum of the particle of mass \sqrt{s} into two decay products with equal mass m in its rest frame.

References

- [1] Matthias Neubert and Berthold Stech. Nonleptonic weak decays of B mesons. *Adv. Ser. Direct. High Energy Phys.*, 15:294–344, 1998.

- [2] Peter Lichard. Are the production and decay of a resonance always independent? *Acta Phys. Slov.*, 49:215–230, 1999.
- [3] Nathan Isgur, Colin Morningstar, and Cathy Reader. The a_1 in tau Decay. *Phys. Rev.*, D39:1357, 1989.
- [4] Alan Weinstein. Breit Wigners and Form Factors CBX 99-55 (Unpublished report) September 1999
- [5] Charles Zemach. Determination of the Spins and Parities of Resonances. *Phys. Rev.*, 140:B109–B124, 1965.
- [6] Charles Zemach. Use of angular momentum tensors. *Phys. Rev.*, 140:B97–B108, 1965.
- [7] C. Tanabashi et al. Review of Particle Physics. *Phys. Rev. D*, **98**, 030001 (2018).
- [8] A. Kuzmin *et al.* [Belle Collaboration], *Phys. Rev. D* **76** (2007) 012006.
- [9] B. Aubert *et al.* [BaBar Collaboration], *Phys. Rev. D* **75**, 031101 (2007).
- [10] B. Aubert *et al.* [BaBar Collaboration], *Phys. Rev. D* **74**, 111102 (2006).
- [11] K. Abe *et al.* [Belle Collaboration], *Phys. Rev. D* **69** (2004) 112002 doi:10.1103/PhysRevD.69.112002 [hep-ex/0307021].
- [12] P. del Amo Sanchez *et al.* [BaBar Collaboration], *PoS ICHEP 2010* (2010) 250 [arXiv:1007.4464 [hep-ex]].
- [13] R. Aaij *et al.* [LHCb Collaboration], *Phys. Rev. D* **92** (2015) 3, 032002 doi:10.1103/PhysRevD.92.032002 [arXiv:1505.01710 [hep-ex]].
- [14] R. Aaij *et al.* [LHCb Collaboration], *Phys. Rev. D* **94** (2016) no.7, 072001 doi:10.1103/PhysRevD.94.072001 [arXiv:1608.01289 [hep-ex]].
- [15] B. Aubert *et al.* [BaBar Collaboration], *Phys. Rev. D* **79** (2009) 112004 doi:10.1103/PhysRevD.79.112004 [arXiv:0901.1291 [hep-ex]].
- [16] V. Morenas, A. Le Yaouanc, L. Oliver, O. Pene, J.C. Raynal, *Phys.Rev. D*56 (1997) 5668-5680, hep-ph/9706265
See also the more recent discussion and references in Alain Le Yaouanc, Olivier Pène, *Int.J.Mod.Phys. A*30 (2015) no.10, 1543009, arXiv:1408.5104 [hep-ph]
- [17] D. Liventsev *et al.* [Belle Collaboration], *Phys. Rev. D* **77** (2008) 091503.
- [18] B. Aubert *et al.* [BaBar Collaboration], *Phys. Rev. Lett.* **100** (2008) 151802.
- [19] B. Aubert *et al.* [BaBar Collaboration], *Phys. Rev. Lett.* **101** (2008) 261802.
- [20] N. Isgur and M.Wise, *Phys. Rev. D* **43** (1991) 819.

- [21] T. M. Yan, H. Y. Cheng, C. Y. Cheung, G. L. Lin, Y. C. Lin and H. L. Yu, Phys. Rev. D **46**, 1148 (1992) Erratum: [Phys. Rev. D **55**, 5851 (1997)]. doi:10.1103/PhysRevD.46.1148, 10.1103/PhysRevD.55.5851
- [22] Gourdin, M. and Salin, Ph. Nuovo Cimento 27 (1963) 193
- [23] C. L. Y. Lee, M. Lu and M. B. Wise, Phys. Rev. D **46**, 5040 (1992). doi:10.1103/PhysRevD.46.5040
- [24] G. Kramer and W. F. Palmer, Phys. Lett. B **298**, 437 (1993). doi:10.1016/0370-2693(93)91847-G
- [25] I. Caprini, L. Lellouch and M. Neubert, Nucl. Phys. B **530**, 153 (1998) doi:10.1016/S0550-3213(98)00350-2 [hep-ph/9712417].
- [26] J. L. Goity and W. Roberts, Soft pion emission in semileptonic B meson decays, Phys. Rev. D **51** (1995) 3459, doi:10.1103/PhysRevD.51.3459 [hep-ph/9406236].
- [27] F. U. Bernlochner, Z. Ligeti and S. Turczyk, A Proposal to solve some puzzles in semileptonic B decays, Phys. Rev. D **85** (2012) 094033, doi:10.1103/PhysRevD.85.094033, [arXiv:1202.1834 [hep-ph]].
- [28] B. Aubert *et al.* [BaBar Collaboration], Phys. Rev. D **79** (2009) 012002
- [29] J. P. Lees *et al.* [BaBar Collaboration], Phys. Rev. D **95** (2017) no.7, 072001.
- [30] Y. Amhis *et al.*, arXiv:1612.07233 [hep-ex].